

Slow diffusion is necessary to explain the γ -ray pulsar halos

Li-Zhuo Bao,^{1,2} Kun Fang,^{1,3} and Xiao-Jun Bi^{1,2,3,*}

¹*Key Laboratory of Particle Astrophysics, Institute of High Energy Physics,*

Chinese Academy of Sciences, Beijing 100049, China

²*University of Chinese Academy of Sciences, Beijing 100049, China*

³*TIANFU Cosmic Ray Research Center, Chengdu, 610000 Sichuan, China*

(Dated: July 16, 2021)

It was suggested that the γ -ray halo around Geminga might not be interpreted by slow-diffusion. If the ballistic regime of electron/positron propagation is considered, the Geminga halo may be explained even with a large diffusion coefficient. In this work, we examine this effect by taking the generalized Jüttner propagator as the approximate relativistic Green's function for diffusion and find that the morphology of the Geminga halo can be marginally fitted in the fast-diffusion scenario. However, the recently discovered γ -ray halo around PSR J0622+3749 at LHAASO cannot be explained by the same effect and slow diffusion is the only solution. Furthermore, both the two pulsar halos require a conversion efficiency from the pulsar spin-down energy to the high energy electrons/positrons much larger than 100%, if they are interpreted by this ballistic transport effect. Therefore, we conclude that slow diffusion is necessary to account for the γ -ray halos around pulsars.

* bixj@ihep.ac.cn

I. INTRODUCTION

It has been predicted that a middle-aged pulsar should be surrounded by a γ -ray halo [1]. The γ -ray halo is generated by the high-energy electrons and positrons¹, accelerated by the central pulsar wind nebula (PWN), scattering with the background photons when they are injected and propagate in the interstellar medium. The γ -ray halos around Geminga and Monogem were first detected by the HAWC Collaboration [2]. The most intriguing feature of the halos is that the diffusion coefficients indicated by the γ -ray profiles are much smaller than the average value in the Galaxy derived by the B/C data.

Recently, a paper by Recchia et al. [3] points out another plausible scenario, in which the pulsar halo may be explained without a slow-diffusion environment. It is well known that the non-relativistic diffusion equation has the superluminal problem. For the relativistic particles injected within the time $t_{\text{crit}} \equiv 3D/c^2$, the typical diffusion distance $\lambda \sim \sqrt{Dt}$ is greater than ct , where D is the diffusion coefficient and c is the light speed. For $t \ll t_{\text{crit}}$, the particles should propagate ballistically rather than diffusively. They found that the ballistic propagation and the transition to the diffusion regime may explain the Geminga halo even assuming a typical diffusion coefficient in the Galaxy.

The superluminal problem in non-relativistic diffusion equation has been studied in Ref. [4]. It is found that the generalized Jüttner propagator can be taken as the approximate relativistic Green's function for diffusion although a full relativistic diffusion equation has not been developed [4]. The method used in Ref. [3] can be considered as an approximate form of the Jüttner propagator to describe the ballistic and quasi-ballistic propagation.

In this work, we examine the effect of relativistic diffusion on the interpretation of the γ -ray pulsar halos. We adopt the generalized Jüttner propagator as the relativistic Green's function for the diffusion equation. Besides the Geminga halo that has been paid great attention, we also test another newly discovered γ -ray halo around PSR J0622+3749 by LHAASO-KM2A [5], which is very likely an analog of the Geminga halo.

We find that if the effect of ballistic propagation is taken into account the profile of the γ -ray halo around Geminga can be roughly fitted and the result of Ref. [3] is repeated. However, the same effect can not account for the γ -ray halo profile around J0622+3749 and slow diffusion is still necessary in this case. Furthermore, for the large diffusion coefficients the conversion efficiencies

¹ For simplicity, we use *electrons* to denote both electrons and positrons hereafter.

from pulsar spin-down energy to the high energy electrons are much greater than 100% for both the two halos.

In the next section, we will present our calculation and the results. Then we give the conclusion.

II. CALCULATION AND RESULTS

Pulsar halos are generated by electrons escaping from the PWNe and wandering in the ISM. Thus, solving the electron propagation equation in the ISM is the core of calculating the halo morphology. The electron propagation can be expressed by the diffusion-cooling equation:

$$\frac{\partial N(E, \mathbf{r}, t)}{\partial t} = D(E)\Delta N(E, \mathbf{r}, t) + \frac{\partial [b(E)N(E, \mathbf{r}, t)]}{\partial E} + Q(E, \mathbf{r}, t), \quad (1)$$

where E is the electron energy and N is the electron number density. The diffusion coefficient is taken as $D(E) = D_0(E/1 \text{ GeV})^\delta$, where we assume $\delta = 1/3$ following the Komolgorov's theory.

The energy-loss rate is defined by $b(E) = -dE/dt$ and can be expressed by $b(E) = b_0 E^2$. ICS and synchrotron radiation dominate the energy losses of high-energy electrons. Considering the Klein-Nishina effect in ICS, b_0 should be energy dependent. We adopt the parameterization given by Ref. [6] to precisely calculate the ICS component. The seed photon fields for ICS are taken from Ref. [2] and [7] for Geminga and LHAASO J0621+3755, respectively. We take the magnetic field to be $3 \mu\text{G}$ for both the cases to get the synchrotron component.

The source function is taken as

$$Q(E, \mathbf{r}, t) = \begin{cases} q(E) \delta(\mathbf{r} - \mathbf{r}_s) (1 + t/t_{\text{sd}})^{-2} / (1 + t_s/t_{\text{sd}})^{-2}, & t \geq 0 \\ 0, & t < 0 \end{cases}, \quad (2)$$

where $q(E)$ is the electron injection spectrum at the current time, \mathbf{r}_s is the position of the pulsar, t_s is the pulsar age, and t_{sd} is the typical spin-down time scale of pulsar, which is set to be 10 kyr.

We assume the injection spectrum to be a power-law form with an exponential cutoff:

$$q(E) = q_0 (E/1 \text{ GeV})^{-p} \exp[-(E/E_c)^\alpha], \quad (3)$$

where p , E_c , and α are listed in Table. I, and the normalization q_0 can be determined by the relation

$$\int q(E) E dE = \eta L, \quad (4)$$

where L is the current spin-down luminosity of the pulsar and η is the conversion efficiency from the spin-down energy to the electron energy. For the Geminga halo, the spectral parameters

are determined by a roughly fit to a preliminary γ -ray spectrum of HAWC [8]. For LHAASO J0621+3755, we adopt the best-fit spectral parameters to the LHAASO-KM2A spectrum [5, 7].

We can obtain the solution of Eq. (1) with the Green's function method:

$$N(E, \mathbf{r}, t) = \int_{\mathbf{R}^3} d^3\mathbf{r}_0 \int_{-\infty}^t dt_0 \int_{-\infty}^{+\infty} dE_0 G(E, \mathbf{r}, t; E_0, \mathbf{r}_0, t_0) Q(E_0, \mathbf{r}_0, t_0). \quad (5)$$

In the normal diffusion model, the Green's function is expressed as

$$G(E, \mathbf{r}, t; E_0, \mathbf{r}_0, t_0) = \frac{1}{b(E)(\pi\lambda^2)^{3/2}} \exp\left[-\frac{(\mathbf{r} - \mathbf{r}_0)^2}{\lambda^2}\right] \delta(t - t_0 - \tau) H(\tau), \quad (6)$$

where

$$\lambda = 2 \sqrt{\int_E^{E_0} \frac{D(E')}{b(E')} dE'}, \quad \tau = \int_E^{E_0} \frac{dE'}{b(E')}, \quad (7)$$

and H is the Heaviside step function.

In order to eliminate superluminal motion, we need to find the relativistic correction of Eq. (1). Unfortunately, many efforts over decades have not been successful so far. To evade this difficulty, Dunkel et al. [9] noticed that the propagator

$$P(E, x, t) = \frac{1}{(\pi\lambda^2)^{3/2}} \exp\left(-\frac{x^2}{\lambda^2}\right) \quad (8)$$

has the same form with the Maxwell-Boltzmann speed distribution of particles with mass m in thermal equilibrium gas with temperature T :

$$f_{M-B}(\mathbf{v}) = \left(\frac{m}{2\pi kT}\right)^{3/2} \exp\left(-\frac{m\mathbf{v}^2}{2kT}\right), \quad (9)$$

if we make the replacements $v \rightarrow x$ and $2kT/m \rightarrow \lambda^2$. Jüttner [10] derived the Maxwell-Jüttner distribution which describes the speeds of relativistic particles in thermal equilibrium gas:

$$f_{M-J}(\mathbf{p}) = \frac{1}{4\pi(mc)^3} \frac{\mu}{K_2(\mu)} \exp(-\gamma\mu), \quad (10)$$

where $\mathbf{p} = \gamma m\mathbf{v}$ represents the momentum, $\gamma = 1/\sqrt{1 - v^2/c^2}$ represents the Lorentz factor, $\mu = mc^2/kT$, and K_ν is the ν -order modified Bessel function of the second kind. From the relationship $4\pi v^2 f_v(\mathbf{v}) dv = 4\pi p^2 f_p(\mathbf{p}) dp$, we derive

$$f_{M-J}(\mathbf{v}) = \frac{\gamma^5}{4\pi c^3} \frac{\mu}{K_2(\mu)} \exp(-\gamma\mu). \quad (11)$$

However, the standard form Eq. (11) might not represent the correct relativistic equilibrium distribution [11]. A modification

$$f_{M-J}(\mathbf{v}) = \frac{\gamma^4}{4\pi c^3} \frac{\mu}{K_1(\mu)} \exp(-\gamma\mu) \quad (12)$$

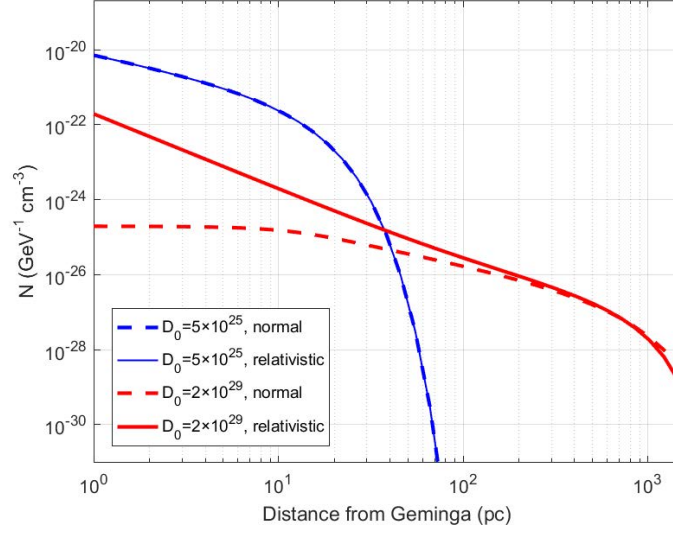


FIG. 1. Electron number densities as functions of the distance from Geminga for the slow-diffusion ($D_0 = 5 \times 10^{25} \text{ cm}^2 \text{ s}^{-1}$) and fast-diffusion ($D_0 = 2 \times 10^{29} \text{ cm}^2 \text{ s}^{-1}$) scenarios. Both the relativistic and non-relativistic diffusion models are presented. The conversion efficiency is set as 100% for all the cases in this figure.

is most frequently suggested.

It reminds us to take Eq. (12) with the same replacements $v \rightarrow x$, $2kT/m \rightarrow \lambda^2$ and $c \rightarrow ct$ as the propagator in the Green's function, called the generalized Jüttner propagator [4]:

$$P_{\text{rela}}(E, x, t) = \frac{1}{4\pi(ct)^3} \frac{H[1 - \xi(x, t)]}{[1 - \xi^2(x, t)]^2} \frac{\kappa(E, t)}{K_1[\kappa(E, t)]} \exp\left[-\frac{\kappa(E, t)}{\sqrt{1 - \xi^2(x, t)}}\right], \quad (13)$$

where $\xi(r, t) = x/ct$ and $\kappa(E, t) = 2(ct/\lambda)^2$. The Heaviside step function H is used to ensure that P_{rela} vanishes when $r > ct$. In the extreme case of $\kappa \ll 1$ or $\kappa \gg 1$, the propagator will transit to ballistic or diffusive propagator separately (see Appendix A). In this way we derive the Green's function with relativistic correction:

$$G_{\text{rela}}(E, \mathbf{r}, t; E_0, \mathbf{r}_0, t_0) = \frac{1}{4\pi[c(t - t_0)]^3 b(E)} \frac{H(1 - \xi)}{(1 - \xi^2)^2} \frac{\kappa}{K_1(\kappa)} \exp\left(-\frac{\kappa}{\sqrt{1 - \xi^2}}\right) \delta(t - t_0 - \tau) H(\tau), \quad (14)$$

where $\xi = (\mathbf{r} - \mathbf{r}_0)/c(t - t_0)$ and $\kappa = 2[c(t - t_0)/\lambda]^2$.

In Fig. 1, we draw N as functions of the distance from Geminga to show the effect of relativistic correction. The electron energy is 100 TeV, which is roughly the parent electron energy of the TeV pulsar halos. The conversion efficiency is set as 100% for all the cases. As expected, there

is little difference between the standard and relativistic diffusion models in the slow-diffusion scenario. When the diffusion coefficient is significantly larger, the relativistic correction is crucial. The newly injected electrons are still in the ballistic regime and cannot flee far away from the source with superluminal velocities, leading to a more constrictive distribution than that of the non-relativistic case. However, although the fast-diffusion scenario can also predict a steep electron distribution near the source after the relativistic correction, the absolute N is about an order of magnitude smaller than that of the slow-diffusion scenario. It means that a significantly larger conversion efficiency is required for the former to explain a same observation.

We integrate N over the line of sight from the Earth to an angle of θ observed away from the pulsar to get the electron surface density and then obtain the γ -ray surface brightness profile (SBP) with the standard calculation of ICS [12]. For the case of LHAASO J0621+3755, the point-spread function (PSF) must be considered, which is a Gaussian function with a size of 0.45° .

We vary the diffusion coefficient D_0 from 10^{25} to 10^{30} $\text{cm}^2 \text{s}^{-1}$ and take the energy conversion efficiency η as the free parameter to fit the HAWC data for Geminga and the LHASSO-KM2A data for LHAASO J0621+3755, using the least- χ^2 method. Other determined parameters are summarized in Table. I.

TABLE I. Model parameters for Geminga and LHAASO J0621+3755.

	Geminga	J0621
t_s (kyr)	342	208
r_s (pc)	250	1600
L (erg s^{-1})	3.2×10^{34}	2.7×10^{34}
p	1.0	1.5
α	1.0	2.0
E_c (TeV)	150	265

We illustrate the fitting results in Fig. 2. It is clear that there are two minimal values of χ^2 for the Geminga case. The solution of the slow-diffusion scenario with $D_0 = 10^{26}$ $\text{cm}^2 \text{s}^{-1}$ gives very good fit to the data with $\chi^2/\text{d.o.f.} \sim 1$. The fast-diffusion scenario with $D_0 = 2 \times 10^{29}$ $\text{cm}^2 \text{s}^{-1}$ also gives an acceptable fit, which is in agreement with the result of Ref. [3]. The latter diffusion coefficient is consistent with the Galactic typical value derived by B/C data [13]. The required η for the slow-diffusion scenario is $\sim 5\%$, while the fast-diffusion scenario needs a conversion

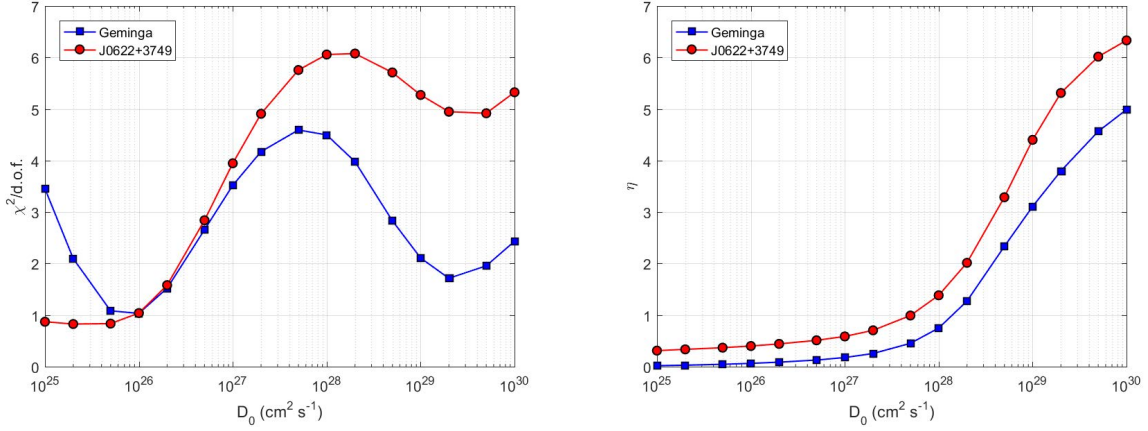


FIG. 2. Left: The minimal χ^2 of best fitting to the γ -ray halo profiles as function of diffusion coefficient at 1 GeV. Right: The efficiency of energy transfer from the pulsar spin-down energy to electron/positron pairs for different values of D_0 .

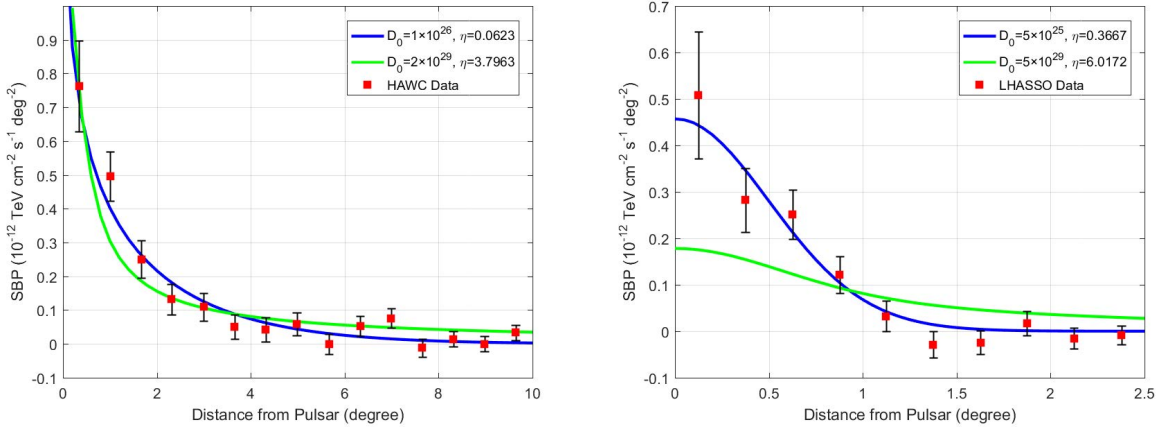


FIG. 3. The γ -ray profiles of the Geminga halo (left) and LHAASO J0621+3755 (right) taking D_0 corresponding to the two local minimal χ^2 .

efficiency of $\sim 400\%$. This value may not be reasonable even considering the uncertainties of the pulsar spin-down luminosity and the required total electron energy.

There are also two local minimal χ^2 for the case of LHAASO J0621+3755. However, only the slow-diffusion solution can fit the LHAASO-KM2A data. The minimal $\chi^2/\text{d.o.f.}$ in the fast-diffusion regime is about 5, corresponding an exclusion with more than 5σ significance. The problem of conversion efficiency is also serious for the fast-diffusion solution.

In Fig. 3, we show the theoretical SBPs corresponding to the two local minimal χ^2 for both the

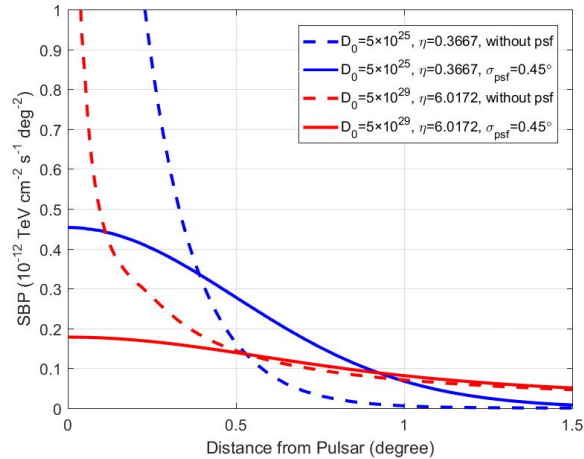


FIG. 4. Comparison of the γ -ray profiles for LHAASO J0621+3755 before and after PSF convolution.

Geminga halo and LHAASO J0621+3755. As already indicated by the χ^2 test, the fast-diffusion scenario can roughly fit the measured SBP of the Geminga halo, while gives a very poor fit to that of LHAASO J0621+3755. The predicted SBP is systematically lower than the data within $\sim 1^\circ$ from the pulsar and higher outside.

To understand the reason that the γ -ray profile of LHAASO J0621+3755 can not be well fitted we show the γ -ray profiles for LHAASO J0621+3755 with/without PSF convolution in solid/dash lines in Fig. 4. For both slow-diffusion and fast-diffusion scenarios, η is set to be the same value of SBP blurred by a Gaussian function with a size of 0.45° (in solid lines). The trends of the two dash lines are similar to those of Geminga. In the case of fast diffusion, the red dash line decreases more steeply in a small region around the pulsar than the blue dash line correspond to slow diffusion scenario, and retains a higher level in the distance because of the constant amount of electrons. Therefore, the red solid line becomes flatter after PSF convolution, and cannot fit the data as well as the blue solid line.

III. CONCLUSION

With a relativistic correction to the electron propagation equation, we examine if the morphologies of pulsar halos can be explained under the fast diffusion scenario, i.e., the typical diffusion coefficient in the Galaxy.

We find that the fast-diffusion scenario can give an acceptable fit to the γ -ray profile of the Geminga halo, which is in agreement with the result of Ref. [3]. In relativistic diffusion, the

propagation of newly injected electrons is ballistic, leading to a steep γ -ray profile near the source similar to the measurement. However, the required η is 400%, which is too large. For LHAASO J0621+3755, the fast diffusion scenario can not give reasonable fit to the profile. Therefore, the fast-diffusion scenario is strongly disfavored even with a relativistic correction.

In comparison, the slow-diffusion scenario can well fit the profiles with reasonable η for both the two halos. Furthermore, the slow-diffusion assumption also matches the symmetry of the Geminga halo. If the diffusion coefficient is as large as the Galactic average, the mean free path of electrons at 100 TeV reaches tens of parsecs, which very likely corresponds to strong asymmetries of the halo [14]. All these indicate that slow diffusion is still necessary to interpret pulsar halos.

Appendix A: Discussion on the Extreme Cases of Generalized Jüttner Propagator

In the case of $\lambda \gg ct$, we have $\kappa \ll 1$ and

$$\frac{\kappa}{K_1(\kappa)} \approx \kappa^2. \quad (\text{A1})$$

Substituting Eq.(A1) into Eq.(13), we have

$$P_{\text{rela}}(E, x, t) \approx \frac{1}{4\pi(ct)^3} \frac{H(1-\xi)}{(1-\xi^2)^2} \kappa^2 \exp\left(-\frac{\kappa}{\sqrt{1-\xi^2}}\right) = \frac{H(1-\xi)}{4\pi(ct)^3} \frac{ydy}{\xi d\xi} \exp(-y), \quad (\text{A2})$$

where $y = \kappa / \sqrt{1-\xi^2}$.

The ballistic propagator is written as

$$P_{\text{ball}}(E, x, t) = \frac{1}{4\pi c^3 t^2} \delta(ct - x). \quad (\text{A3})$$

By evaluating the integral of Eq.(A3) multiplied by any function q of t , we have

$$\int_{-\infty}^{+\infty} G_{\text{ball}}(E, x, t) q(t) dt = \frac{1}{4\pi c x^2} q\left(\frac{x}{c}\right). \quad (\text{A4})$$

Applying the same operation to Eq.(A2), we obtain

$$\begin{aligned} \int_{-\infty}^{+\infty} P_{\text{rela}}(E, x, t) q(t) dt &\approx \int_{\frac{x}{c}}^{+\infty} \frac{1}{4\pi(ct)^3} \frac{ydy}{\xi d\xi} \exp(-y) q(t) dt \\ &= \int_0^{+\infty} \frac{1}{4\pi(ct)^3} \frac{x}{c\xi^3} y \exp(-y) q[t(y)] dy \\ &= \frac{1}{4\pi c x^2} \int_0^{+\infty} y \exp(-y) q[t(y)] dy, \end{aligned} \quad (\text{A5})$$

which coincides with Eq.(A4) because $\int_0^{+\infty} y \exp(-y) dy = 1$ and the approximation

$$t(y) = \frac{x}{c \sqrt{1 - (\frac{\kappa}{y})^2}} \approx \frac{x}{c} \quad (\text{A6})$$

holds on the main part of integral interval.

In the case of $\lambda \ll ct$, we have $\kappa \gg 1$ and

$$\frac{\kappa}{K_1(\kappa)} \approx \sqrt{\frac{2}{\pi}} \kappa^{3/2} \exp(\kappa). \quad (\text{A7})$$

At a distance $x \lesssim \lambda$ where the electron number density is non-ignorable, we obtain

$$\xi = \frac{x}{ct} \lesssim \frac{\lambda}{ct} \ll 1. \quad (\text{A8})$$

Substituting Eq.(A7) and the first-order approximations $1/(1 - \xi^2)^2 \approx 1$ and $\exp(-\kappa/\sqrt{1 - \xi^2}) \approx \exp[-\kappa(1 + \xi^2/2)]$ into Eq.(13), we have

$$P_{\text{rela}}(E, x, t) \approx \frac{1}{(ct)^3} \frac{1}{(1 - \xi^2)^2} \left(\frac{\kappa}{2\pi}\right)^{3/2} \exp\left(-\frac{\kappa\xi^2}{2}\right) = \frac{1}{(\pi\lambda^2)^{3/2}} \exp\left(-\frac{x^2}{\lambda^2}\right), \quad (\text{A9})$$

which coincides with Eq.(8), indicating that the propagator transits to the normal one.

ACKNOWLEDGMENTS

This work is supported by the National Natural Science Foundation of China under the grant No. U1738209.

-
- [1] T. Linden, K. Auchetl, J. Bramante, I. Cholis, K. Fang, D. Hooper, T. Karwal, and S. W. Li, *Phys. Rev. D* **96**, 103016 (2017), 1703.09704.
 - [2] A. Abeysekara et al. (HAWC), *Science* **358**, 911 (2017), 1711.06223.
 - [3] S. Recchia, M. Di Mauro, F. A. Aharonian, F. Donato, S. Gabici, and S. Manconi (2021), 2106.02275.
 - [4] R. Aloisio, V. Berezhinsky, and A. Gazizov, *Astrophys. J.* **693**, 1275 (2009), 0805.1867.
 - [5] F. Aharonian, Q. An, L. Bai, Y. Bai, Y. Bao, D. Bastieri, X. Bi, Y. Bi, H. Cai, J. Cai, et al., *Phys. Rev. Lett.* **126**, 241103 (2021).
 - [6] K. Fang, X.-J. Bi, S.-J. Lin, and Q. Yuan, *Chin. Phys. Lett.* **38**, 039801 (2021), 2007.15601.
 - [7] K. Fang, S.-Q. Xi, and X.-J. Bi (2021), 2107.02140.

- [8] H. Zhou, in 36th International Cosmic Ray Conference (ICRC2019) (2019), vol. 36 of International Cosmic Ray Conference, p. 832.
- [9] J. Dunkel, P. Talkner, and P. Hänggi, *Phys. Rev. D* **75**, 043001 (2007).
- [10] F. Jüttner, *Annalen der Physik* **339**, 856 (1911).
- [11] J. Dunkel, P. Talkner, and P. Hänggi, *New J. Phys.* **9**, 144 (2007).
- [12] G. Blumenthal and R. Gould, *Rev. Mod. Phys.* **42**, 237 (1970).
- [13] Q. Yuan, S.-J. Lin, K. Fang, and X.-J. Bi, *Phys. Rev. D* **95**, 083007 (2017), 1701.06149.
- [14] R. López-Coto and G. Giacinti, *Mon. Not. Roy. Astron. Soc.* **479**, 4526 (2018), 1712.04373.